MNRAS 000, 1–8 (2017) Preprint 3 October 2017 Compiled using MNRAS LATEX style file v3.0

SN-BHM: A hierarchical Bayesian model for Supernova Cosmology

Samuel R. Hinton,[1,2]★ Alex G. Kim,[3] Tamara M. Davis[1,2]
[1]*School of Mathematics and Physics, The University of Queensland, Brisbane, QLD 4072, Australia*
[2]*ARC Centre of Excellence for All-sky Astrophysics (CAASTRO)*
[3]*Physics Division, Lawrence Berkeley National Laboratory, 1 Cyclotron Road, Berkeley, CA 94720, USA*

Accepted XXX. Received YYY; in original form ZZZ

ABSTRACT
Abstract Abstract

Key words: keyword1 – keyword2 – keyword3

1 INTRODUCTION

Almost two decades have passed since the discovery of the accelerating universe (Riess et al. 1998; Perlmutter et al. 1999). Since that time, of the number of observed Type Ia supernovae (SN Ia) have increased by more than an order of magnitude thanks to modern surveys at both low redshift (Bailey et al. 2008; Freedman et al. 2009; Hicken et al. 2009; Contreras et al. 2010; Conley et al. 2011), and higher redshift (Astier et al. 2006; Wood-Vasey et al. 2007; Balland et al. 2009; Amanullah et al. 2010). Cosmological analysis of these supernova samples (Kowalski et al. 2008; Conley et al. 2011; Suzuki et al. 2012; Betoule et al. 2014; Rest et al. 2014) have been combined with complimentary probes of large scale structure (Alam et al. 2017) and the CMB (Hinshaw et al. 2013; Planck Collaboration et al. 2013), and yet, despite these prodigious efforts, the nature of dark energy remains an unsolved mystery.

In attempts to tease out the nature of dark energy, currently running and planned surveys are once again ramping up their statistical power. The Dark Energy Survey (DES, Bernstein et al. 2012; Abbott et al. 2016) will be observing thousands of Type Ia supernova, attaining both spectroscopic and photometric confirmation. The Large Synoptic Survey Telescope (LSST, Ivezic et al. 2008; LSST Science Collaboration et al. 2009) will produce scores of thousands of photometrically classified supernovae. Such increased statistical power demands a similarly increased fidelity and flexibility in modelling the supernovae for cosmological purposes, as systematic uncertainty will prove to be the limiting factor in our analyses.

As such, staggering effort is being put into developing more sophisticated supernovae analyses. Scolnic & Kessler (2016) and Kessler & Scolnic (2017) explore sophisticated simulation corrections to traditional analyses. Approximate Bayesian computation methods also make use of simulations, trading traditional likelihoods and analytic approximations for more robust models with only the cost of increased computational time (Weyant et al. 2013; Jennings et al. 2016). Hierarchical Bayesian Models abound (Mandel et al. 2009; March et al. 2011, 2014; Rubin et al. 2015; Shariff et al. 2016; Roberts et al. 2017), however often face difficulties finding sufficient analytic approximations for complicated effects such as Malmquist bias.

In this paper, we lay out a new hierarchical model that extends on past work. Section 2 is dedicated to a quick review of the supernovae cosmology. In Section 3 we outline our methodology. Model verification on simulated datasets is given in Section 4. Forecasts for the impending DES three year spectroscopic supernova survey are contain in Section **??**. Section 6 investigates the effect of various systematics on our model, and Section **??** provides details on potential areas of improvement and unsuccessful methodologies.

2 REVIEW

Whilst supernova observations take the form of time-series photometric measurements of brightness in many photometric bands, most analyses do not work from these measurements of apparent magnitude and colour. Instead, most techniques fit these observations of magnitude (along with red-

★ E-mail: samuelreay@gmail.com

shift) to a supernova model, with the most widely used being that of the empirical SALT2 model (Guy et al. 2007, 2010). This model is trained separately before fitting the supernovae light curves for the cosmology selected supernova sample (Guy et al. 2010; Mosher et al. 2014). The resulting output from the model is, for each supernova, a characterised amplitude x_0 (which can be converted into apparent magnitude $m_B = -2.5\log(x_0)$), a stretch term x_1 and colour term c, along with a covariance matrix describing the uncertainty on these summary statistics. As such, the product at the end is a (redshift dependent) population of m_B, x_1 and c.

The underlying actual supernova population is not as clear cut, and indeed accurately characterising this population, its evolution over redshift and effects from environment is one of the challenges of supernova cosmology. However, given some modelled underlying population that lives in the redshift dependent space M_B, x_1 and c, the introduction of cosmology into the model is simple – it is encoded in the functional map between those two populations, from apparent magnitude space to absolute magnitude. Specifically, for any given supernova our functional map may take the traditional form:

$$M_B = m_B + \alpha x_1 - \beta c - \mu(z) + \text{corrections}, \tag{1}$$

where α is the stretch correction (Phillips 1993), and β is the colour correction (Tripp 1998) that respectively encapsulate the empirical relation that broader and bluer supernovae are brighter. The corrections term at the end often includes corrections for host galaxy environment, as this has statistically significant effects on supernova properties (Kelly et al. 2010; Lampeitl et al. 2010; Sullivan et al. 2010; D'Andrea et al. 2011; Gupta et al. 2011; Johansson et al. 2013; Rigault et al. 2013; Uddin et al. 2017). The cosmological term, $\mu(z)$ represents the distance modulus, and is precisely known given cosmological parameters and an input redshift.

2.1 Traditional Analyses

Traditional χ^2 analyses such as that found in Kowalski et al. (2008); Conley et al. (2011); Betoule et al. (2014), minimise the difference in distance modulus between the cosmologically predicted values μ_C and the observed distance modulus $\mu_{\rm obs}$, shown respectively below:

$$\mu_C = 5\log\left[\frac{(1+z)r}{10}\right] \tag{2}$$

$$r = \frac{c}{H_0}\int_0^z \frac{dz'}{\sqrt{\Omega_m(1+z')^3 + \Omega_k(1+z')^2 + \Omega_\Lambda(1+z')^{3(1+w)}}} \tag{3}$$

$$\mu_{\rm obs} = m_B + \alpha x_1 - \beta c - M_B \tag{4}$$

The minimising function is then given as

$$\chi^2 = (\mu_{\rm obs} - \mu_C)^\dagger C^{-1} (\mu_{\rm obs} - \mu_C) \tag{5}$$

where C^{-1} is an uncertainty matrix which combined the uncertainty from the SALT2 fits, intrinsic dispersion, calibration, dust, peculiar velocity and many other factors (see Betoule et al. (2014) for a review). The benefit this analysis methodology provides is speed - for samples of hundreds of supernova, efficient matrix inversion algorithms allow the likelihood to be evaluated quickly. The speed comes with two costs. Firstly, formulating a χ^2 likelihood requires a loss of model flexibility by building into the model assumptions of uncertainty Gaussianity. Secondly, the computational efficiency is dependent on inverting a covariance matrix with dimensionality linearly proportional to the number of supernovae. As this number increases, the cost of inversion rises quickly, and is not viable for samples with thousands of supernovae.

Selection efficiency, such as the well known Malmquist bias (Malmquist K. G. 1922) is accounted for by correcting data. Simulations following survey observational strategies and geometry and used to calculate the expected bias in distance modulus, which is then added onto the observational data.

2.2 Approximate Bayesian Computation

To try and escape the limitations of the traditional analysis methodology, several recent methods have adopted Approximate Bayesian Computation, where supernova samples are forward modelled in parameter space and compared to observed distributions. Weyant et al. (2013) provides an introduction into ABC methods for supernova cosmology in the context of the SDSS-II results (Sako et al. 2014) and Flat ΛCDM cosmology, whilst Jennings et al. (2016) demonstrates their *superABC* method on simulated first season Dark Energy Survey samples, described in Kessler et al. (2015). In both examples, the supernova simulation package SNANA (Kessler et al. 2009) is used to forward model the data at each point in parameter space.

By building the systematic uncertainties and selection effects into the simulation package, there is vastly more freedom in how to treat and model those effects. Data does not need to be corrected, analytic approximations do not need to be applied, we are free to incorporate algorithms which simply cannot be expressed in a tractable likelihood. This freedom comes with a cost – computation. The classical χ^2 method's most computationally expensive step in a fit is matrix inversion. For ABC methods, we must instead simulate an entire supernova population in its entirety – drawing from underlying supernova populations, modelling light curves, applying selection effects, fitting light curves and applying data cuts. This is an intensive process. Luckily, efficient sampling algorithms that have walkers which rely on the Markov properties of groups instead of individual walkers, such as Ensemble sampling (Foreman-Mackey et al. 2013) allow easy parallelisation of parameter fits, such as used in the BAMBIS framework CITE RACHEL.

One final benefit of ABC methods is that they can move past the traditional treatment of supernovae with summary statistics (m_B, x_1 and c). Jennings et al. (2016) presents both a metric used to compare forward modelled summary statistic populations (denoted the 'Tripp' metric) and a metric directly applicable to the observed supernova light curves themselves, however evaluation of systematic uncertainty was only performed using the Tripp metric.

2.3 Hierarchical Bayesian Models

Sitting comfortably between the traditional models simplicity and the complexity of forward modelling lies Hierarchical

Bayesian Models. With the introduction of multiple layers in our model, we can add far more flexibility than a traditional analysis whilst still maintaining most of the computational benefits that come from having a tractable likelihood. Mandel et al. (2009) and Mandel et al. (2011) construct a hierarchical model which they apply to the light curve fitting for supernova. March et al. (2011, 2014); Karpenka (2015) derive a hierarchical model and simplify it by analytically marginalising over nuisance parameters provide a model which offers increased flexibility with reduced uncertainty over the traditional method. The recent BAHAMAS model (Shariff et al. 2016) builds off this and reanalyses the JLA dataset, whilst including extra freedom in the correction factors α and β, finding evidence for redshift dependence on β. Ma et al. (2016) also performed a reanalysis of the JLA dataset, finding significant difference in α and β values from the original as well. Notably, these methods rely on data that is bias corrected, however the UNITY framework given by Rubin et al. (2015) incorporates selection efficiency analytically in the model, and is applied to the Union 2.1 dataset (Suzuki et al. 2012). The well known BEAMS (Bayesian estimation applied to multiple species) methodology from Kunz et al. (2007) has been extended and applied in several works (Hlozek et al. 2012), mostly lately to include redshift uncertainty for photometric redshift application as zBEAMS (Roberts et al. 2017).

The flexibility afforded by a hierarchical model allows for investigations into different treatments of underlying populations, rates, redshift distributions, mass corrections and redshift evolution, each of will will be discussed further in the outline of our model below.

3 OUR METHOD

We construct our Bayesian Hierarchical Model with several goals in mind: creation of a redshift dependent correlated underlying supernova population, increased treatment of systematics, and analytic correction of selection effects. As this is closest to the UNITY method from Rubin et al. (2015, hereafter denoted R15), we follow a similar model scaffold, and construct the model in Stan (Carpenter et al. 2017; Stan Development Team 2017) which uses automatic differentiation and the no-U-turn Sampler (NUTS), which is a variant of Hamiltonian Monte Carlo, to efficiently sample high dimensional parameter space.

At the most fundamental level, a supernova analysis is simply a mapping from an underlying population onto an observed population, where cosmology is encoded directly in the mapping function. The difficulty arises in adding sufficient, physically motivated flexibility in both of these populations whilst not adding *too* much flexibility, such that model fitting becomes pathological due to increasing parameter degeneracies within the model.

3.1 Observed and Latent Population

Like most of the BHM methods introduced previously, we work from the summary statistics as well, where each observed supernova has an apparent magnitude $\hat{m_B}$, stretch $\hat{x_1}$ and colour $\hat{c}$, with uncertainty C^{-1} on those values. Additionally, each supernova has an observed redshift $\hat{z}$ and a host galaxy mass associated with it, $\hat{m}$. Given machine learning classifiers to type supernovae, we will also have a probability of being a Type Ia, $\hat{p}$.

The first layer of the hierarchy represents the latent population of m_B, x_1 and c. This can be thought of as the 'true' values for the supernova, and is normally distributed around the observed values such that

$$P(m_B, x_1, c|\hat{m_B}, \hat{x_1}, \hat{c}, C^{-1}) = \mathcal{N}(\{m_B, x_1, c\}|\{\hat{m_B}, \hat{x_1}, \hat{c}\}, C^{-1}). \quad (6)$$

As we are focused on the spectroscopically confirmed DES supernovae for this iteration of the method, we assume the observed redshift $\hat{z}$ is the true redshift z, and the similarly that the observed mass is the true mass m. Whilst the latter is not physically motivated like the redshift measurement, the relatively small contribution of the host galaxy mass to the model makes this an acceptable approximation.

3.2 Underlying Population

The underlying supernova population is often treated with two components - a population distribution in colour and stretch, and intrinsic dispersion. Analytic models often treat the colour and stretch populations with a skew normal and normal, respectively, and have them as independent. Intrinsic dispersion is treated in a variety of manners in other models, from representing it simply as (Gaussian) scatter on the absolute magnitude of the supernova population, to correlated multivariate normal scatter on the combined magnitude, stretch and colour distribution. Additionally, redshift drift of populations' mean colour and stretch will introduce a cosmological bias in our fits unless the population possesses similar ability to change as a function of redshift.

We model the underlying population and intrinsic dispersion together as a redshift dependent multivariate skew normal for each survey. Following R15 we allow the mean colour and stretch to vary over redshift, anchoring four equally spaced redshift nodes spanning the redshift range of each survey, linearly interpolating between the nodes. Both the colour and stretch means are modelled with normal priors. The correlation between the magnitude, stretch and colour populations is represented in a correlation matrix ρ, which is treated with an LKJ prior. Skewness is fixed to 0 for the absolute magnitude population, but left free for colour and stretch, with normal priors centered at 0 to draw the skewness to zero if not well constrained by the data. The decision to include skewness on the stretch distribution as well as the colour was motivated by Scolnic & Kessler (2016), which found highly asymmetric underlying populations for both colour and stretch, regardless of survey or scatter model adopted.

The width of the population, represented by the vector $\{\sigma_{M_B}, \sigma_{x_1}, \sigma_c\}$ is subject to Cauchy priors, however are sampled in log space for efficiency in sampling close to zero.

As such, the only constant between survey populations is the absolute magnitude M_B, with the skewness, redshift dependent means, width and correlations fit individual for each survey.

On top of the Ia populations, as described above, we also include a simplistic outlier population that also follows R15 (and therefore Kunz et al. (2007)) as a Gaussian mixture;

where the mean of the population is fixed to the Ia population, but the population width is set to a width of $\sigma^{\rm outl} = 1$ in M_B, x_1 and c. With the spectroscopic DES sample, the contamination rate is expected to be far too low to actually fit contamination population, however in future works with photometric samples which will suffer from significantly more contamination it will be required that extra degrees of freedom are afforded the outlier population. Proof of concept simulation fits show that an acceptable parameterisation is to represent the typically brighter contaminant population as $\langle M_B^{\rm outl}\rangle = \langle M_B\rangle - \delta_{M_B}^{\rm outl}$, where $\delta_{M_B}^{\rm outl}$ is constrained to be positive, or even to be greater than a small positive number to reduce degeneracy between the two populations. For the purposes of the DES spectroscopic sample which will be dominated by confirmed Type Ia supernovae, $\delta_{M_B}^{\rm outl} = 0$. We assume that supernova fall into either population as determined by their observed classification probability $\hat{p}$.

3.3 Population Map

3.3.1 Cosmology

We formulate our model with three different cosmological parameterisations; Flat ΛCDM, Flat wCDM and standard ΛCDM. Ω_m is given the prior $\mathcal{U}(0.05, 0.99)$, Ω_Λ was treated with $\mathcal{U}(0, 1.5)$ and the equation of state w was similarly set to a flat prior $\mathcal{U}(-0.4, -2.0)$. For calculating the distance modulus, we fix $H_0 = 70 \mathrm{km\,s^{-1}\,Mpc^{-1}}$.

3.3.2 Standardisation Parameters

With increasingly large datasets and more nuanced analyses, the choice of how to handle α and β becomes an important consideration when constructing a model. R15 employs a broken linear relationship for both colour and stretch, where different values of α and β are adopted depending on whether x_1 and c are respectively positive or negative (although the cut could be placed at a location other than 0). Shariff et al. (2016) instead of employing a colour-dependent β, model β as redshift dependent, testing two phenomenological models; $\beta(z) = \beta_0 + \beta_1 z$ and $\beta(z) = \beta_0 + \Delta\beta\,(0.5 + \arctan(100(z - z_t))/\pi)$, where the later effects a rapid but smooth change in β at a turnover redshift z_t.

We tested two models against simulated supernova sets; $\beta(c) = \beta_0 + \beta_1 c$ and $\beta(z) = \beta_0 + \beta_1 z$. See Section 4.2 for details on simulation generation. We found for both models that non-zero values for β_1 are preferred (even with constant β used in simulation) due to severe degeneracy with selection effects. This degeneracy resulted in a significant bias in cosmology, and so in our final model we continue to adopt the constant α and β found in traditional analyses.

3.3.3 Host Galaxy Environment

It is now well known that host galaxy environment has a significant effect on supernova properties. The latest sample of over 1300 spectroscopically confirmed Type Ia supernova show $> 5\sigma$ evidence for correlation between host mass and luminosity (Uddin et al. 2017). The traditional correction, as employed in analyses such as Suzuki et al. (2012) and Betoule et al. (2014) invoke a step function such that $\Delta M = 0.08\mathcal{H}(log(M) - 10))$, where $\mathcal{H}$ is the Heaviside step function and M is the galaxy mass in solar masses. The scale of this step function varies from analysis to analysis, with the 0.08 value shown previously sourced from Sullivan et al. (2010) and used in Betoule et al. (2014). In this work we adopt the model used in R15, which follows the work from Rigault et al. (2013), such that we introduce two parameters to incorporate a redshift-dependent host galaxy mass correction:

$$\Delta M = \delta(0)\left[\frac{1.9\left(1 - \frac{\delta(0)}{\delta(\infty)}\right)}{0.9 + 10^{0.95z}} + \frac{\delta(0)}{\delta(\infty)}\right] \tag{7}$$

We also take flat priors on the parameterisation $\delta(0)$, $\delta(0)/\delta(\infty)$.

3.3.4 Systematics

The chief difficulty with including systematics in supernova analyses is that the generally occur during the observational pipeline, and have difficult to model effects on the output observations. As such, the normal treatment for systematics is to compute their effect on the supernova summary statistics – computing the numerical derivatives $\frac{\partial \hat{m_B}}{\partial Z_i}$, $\frac{\partial \hat{x_1}}{\partial Z_i}$, $\frac{\partial \hat{c}}{\partial Z_i}$, where Z_i represents the $i^{\rm th}$ systematic.

Assuming that the gradients can be linearly extrapolated – which is a reasonable approximation for modern surveys with high quality control of systematics – we can incorporate into our model a deviation from the observed original values by constructing a $(3 \times N_{\rm sys})$ matrix containing the numerical derivatives for the $N_{\rm sys}$ systematics and multiplying it with the row vector containing the offset for each systematic. But scaling the gradient matrix to represent the shift over 1σ of systematic uncertainty, we can simply enforce a unit normal prior on the systematic row vector to increase computational efficiency.

This method of adjusting the observed summary statistics is used throughout the traditional and BHM analyses, however it is normally constrained to band systematics. That is, each band for each survey has two systematics associated with it - the calibration uncertainty and the filter wavelength uncertainty. We include these in our approach, in addition to including HST Calspec calibration uncertainty, 10 SALT2 model systematic uncertainties, three dust systematics (scale, dust model, and transfer law) and also the systematic peculiar velocity uncertainty. This gives fourteen global systematics shared by all surveys, plus two systematics per band in each survey.

3.3.5 Selection Effects

Our treatment of selection effects is to incorporate selection efficiency into our model, rather than relying on simulation-driven data corrections. As such, we need to describe the probability that the events we observe are both drawn from the distribution predicted by the underlying theoretical model *and* that those events, given they happened, are subsequently successfully observed. To make this extra conditional explicit, we can write the likelihood of the data given an underlying model, θ, *and* that the data are included in

our sample, denoted by S, as

$$\mathcal{L} = P(\text{data}|\theta, S). \tag{8}$$

As the model so far described in previous sections describes $P(D|\theta)$, and we wish to formulate a function $P(S|\text{data}, \theta)$ that describes the chance of an event being successfully observed, we rearrange the likelihood in terms of those functions and find

$$\mathcal{L} = \frac{P(S|\text{data}, \theta)P(\text{data}|\theta)}{\int P(S|D, \theta)P(D|\theta)\, dD}, \tag{9}$$

where the denominator represents an integral over all potential data. Full derivation of this can be found in Appendix A. As θ represents the vector of all model parameters, and D represents a vector of all observed variables, this is not a trivial integral. Techniques to approximate this integral, such as Monte-Carlo integration or high dimensional Gaussian processes failed to give tractable posterior surfaces that could be sampled efficiently by HMC. We therefore simplify the integral and approximate the selection effects in apparent magnitude and redshift space independently, such that the denominator, denoted now w for simplicity, is given as

$$w = \int \left[\int P(S|m_B)P(m_B|z, \theta)\, dm_B \right] P(S|z)P(z|\theta)\, dz. \tag{10}$$

We apply two further approximations similar to those made in R15 – that the redshift distribution of the observed supernova reasonably well sample the $P(S|z)P(z|\theta)$ distribution, and that the survey colour and stretch populations can be treated as Gaussian for the purposes of this integral. The population $P(m_B|z, \theta)$ thus becomes $\mathcal{N}(m_B|m_B^*(z), \sigma_{m_B}^*)$, where

$$m_B^*(z) = \langle M_B \rangle + \mu(z) - \alpha\langle x_1(z)\rangle + \beta\langle c(z)\rangle \tag{11}$$

$$\sigma_{m_B}^* = \sigma_{M_B}^2 + (\alpha\sigma_{x_1})^2 + (\beta\sigma_c)^2 + 2(\beta\sigma_{M_B,c} - \alpha\sigma m_B, x_1 - \alpha\beta\sigma_{x_1,c}) \tag{12}$$

What then remains is determining the functional form of $P(S|m_B)$. For the treatment of the DES, we find that the error function which smoothly transitions from some constant efficiency down to zero is sufficient. This similar result has been found by many past surveys (Dilday et al. 2008; Barbary et al. 2010; Perrett et al. 2012; Graur et al. 2013; Rodney et al. 2014) THESE CITATIONS EXACTLY MIRROR RUBIN2015, NOT SURE IF I SHOULD CHANGE THEM. For our treatment of the low redshift surveys included Introduce which lowz surveys earlier on we simplify the model fitting and group all low redshift surveys together. This requires a more complicated selection function than the error function used for DES, however is reasonably well fit with a skew normal. The selection functions were fit to apparent magnitude efficiency ratios calculated from SNANA simulations. The DES survey is thus characterised by $\mu_{\text{DES}} = 22.3$, $\sigma_{\text{DES}} = 0.7$, with the combined low redshift surveys characterised by $\mu_{\text{LowZ}} = 14.1$, $\sigma_{\text{LowZ}} = 1.36$, $\alpha_{\text{LowZ}} = 3.8$.

With the well sampled approximation as specified previously, we can remove the redshift integral in Eq (10) and replace it with a correction for each observed supernova. For the error function (DES) and skew normal selection (LowZ) functions respectively, this correction becomes

$$w_{\text{DES}} = \Phi^c\left(\frac{m_B^* - \mu_{\text{DES}}}{\sqrt{\sigma_{m_B}^{*2} + \sigma_{\text{DES}}^2}}\right) \tag{13}$$

$$w_{\text{LowZ}} = 2\mathcal{N}\left(\frac{m_B^* - \mu_{\text{LowZ}}}{\sqrt{\sigma_{m_B}^{*2} + \sigma_{\text{LowZ}}^2}}\right) \times \Phi\left(\frac{\text{sign}(\alpha_{\text{LowZ}})(m_B^* - \mu_{\text{LowZ}})}{\frac{\sigma_{m_B}^{*2}+\sigma_{\text{LowZ}}^2}{\sigma_{\text{LowZ}}^2}\sqrt{\frac{\sigma_{\text{LowZ}}^2}{\alpha_{\text{LowZ}}^2} + \frac{\sigma_{m_B}^{*2}\sigma_{\text{LowZ}}^2}{\sigma_{m_B}^{*2}+\sigma_{\text{LowZ}}^2}}}\right), \tag{14}$$

where Φ represents the normal CDF function, and Φ^c the complimentary CDF.

4 MODEL VERIFICATION

In order to verify our model we run it through several tests. First, we validate on toy models, verifying that there is not significant cosmological bias in data sets more constraining than the DES spectroscopic sample. We then also generate

4.1 Applied to Toy Spectroscopic Data

We generate simple toy data to validate the basic premise of the model. For both DES and LowZ data we draw from an underlying M_B, x_1, c population and translate into apparent magnitude space using $\Omega_m = 0.3$, $\alpha = 0.14$ and $\beta = 3.1$. Masses are randomly drawn from the interval 0 to 1, and a mass correction with $\delta(0) = 0.08$ and $\delta(0)/\delta(\infty) = 0.5$ included. Independent observational errors of 0.04, 0.2, 0.03 on m_B, x_1 and c (following the mean uncertainty for DES SNANA simulations) are added to create the observables. The results are then passed through the selection effects, where each supernova is only selected based on $P(S|m_B)$, using a skew normal function for the LowZ supernovae and error function for the DES-like supernovae. We draw from each survey simulation until we have 300 LowZ supernovae and 700 DES-like supernovae, representing a statistical sample of greater power than the estimated 250 supernovae for the DES spectroscopic analysis.

The above represents one realisation of data. We test three models (Flat ΛCDM, Flat wCDM, ΛCDM) with 300 realisations and find recovery of underlying cosmology without significant bias. Combined posterior surfaces of 22 realisations are shown in Figures 1, 2, 3, with the statistical distribution of realisations for the Flat ΛCDM cosmology shown in Figure 4. Need a think about which plots to show or good way to merge them

4.2 DES SN data validation

BUT THE BELOW IN THE TESTING AREA

Early analyses often treated intrinsic dispersion simply as scatter in the underlying absolute magnitude of the underlying population, but recent analyses require more a more sophisticated approach. In our development of this model and tests of intrinsic dispersion, we analyse the effects of three different scatter models. The first is simplest model

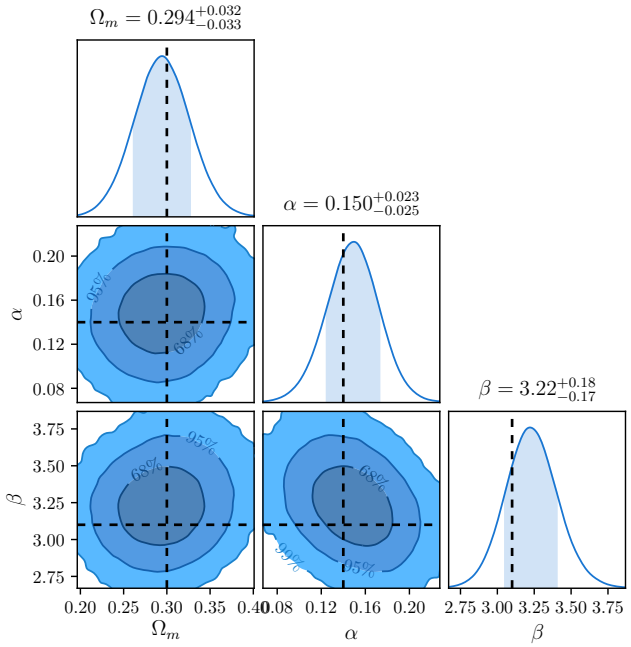

Figure 1. Posterior surfaces for 22 realisations of supernova data with the Flat ΛCDM model.

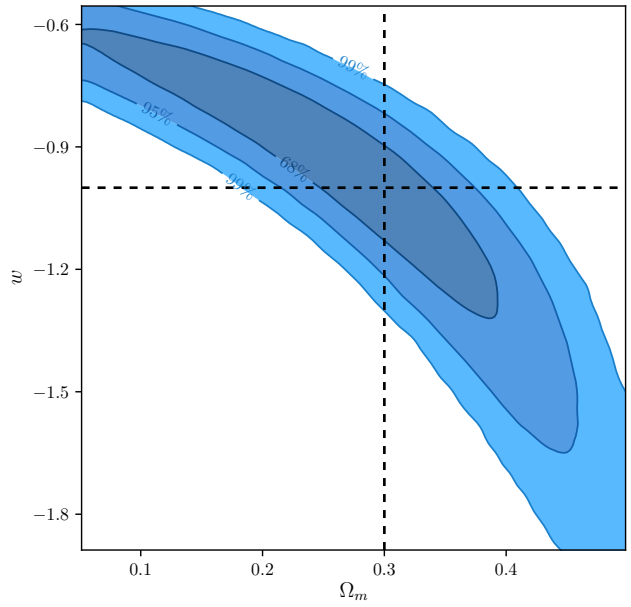

Figure 2. Posterior surfaces for 22 realisations of supernova data with the Flat wCDM model.

- coherent magnitude scatter, denoted 'Smear' in the figures. The second model is the Guy et al. (2010, hereafter denoted the G10 scatter model), which models intrinsic scatter with a 70% contribution from coherent variation and 30% from chromatic variation. The third model, denoted the C11 model is sourced from Chotard et al. (2011) and has variation with 25% contribution from coherent scatter and 75% from chromatic variation.

Simulations (using the SNANA package) follow the observational schedule and observing conditions for the DES and LowZ surveys. In addition to the improvements in the scatter models over the simple data, we also include peculiar velocities for the LowZ sample, and now also include our full treatment of systematics. Additionally, we also simulate two different underlying population – a Gaussian distribution in colour and stretch, and a highly skewed colour and stretch population using population values from Scolnic & Kessler (2016). Both populations have been centered on 0, with the bifurcated Gaussian used for the skewed colour distribution having width $\sigma_c^+ = 0.101$, $\sigma_c^- = 0.043$ and the skewed stretch distribution having $\sigma_{x_1}^+ = 0.222$, $\sigma_{x_1}^- = 1.472$.

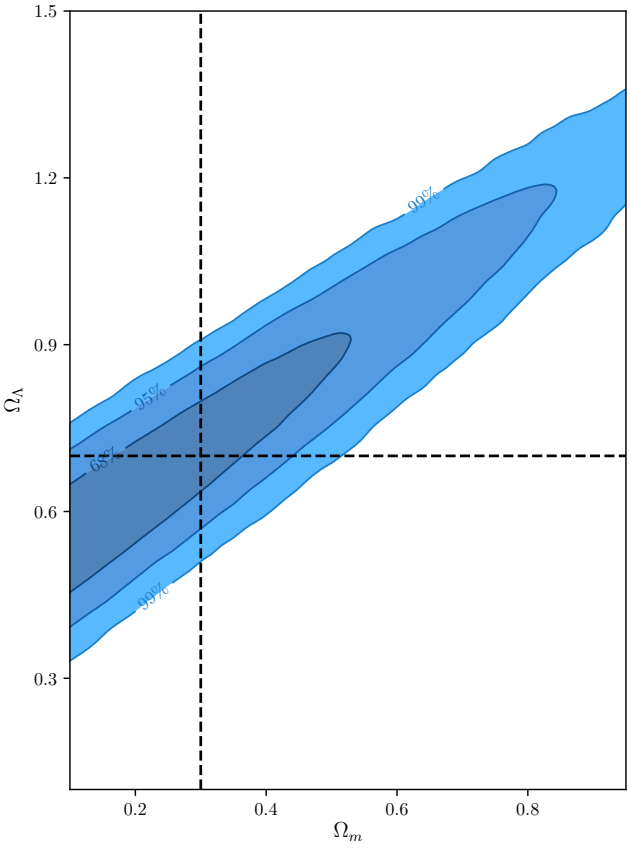

Figure 3. Posterior surfaces for 22 realisations of supernova data with the ΛCDM model.

Each realisation of cosmology fitted contains 300 LowZ supernovae, and 250 DES-like supernovae, such that the uncertainties found when combining chains is representative of the uncertainty in the final DES spectroscopic analysis. Combined posterior surfaces for 20 data realisations are shown in Figure 5. Talk about the biases introduced

UPDATE THIS WHEN THE SIMS FINISH AND I CAN RERUN WITH MORE REALISATIONS

More discussion here when I get more results

5 FORECASTS

Put in multisim forecasts with systamtics both on and off

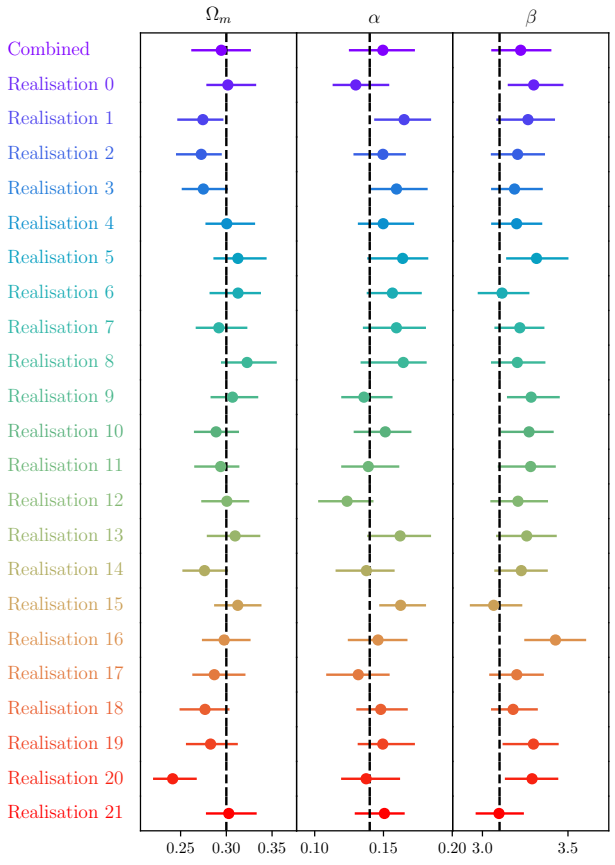

Figure 4. Parameter summaries for 22 realisations of supernova data with the Flat ΛCDM model.

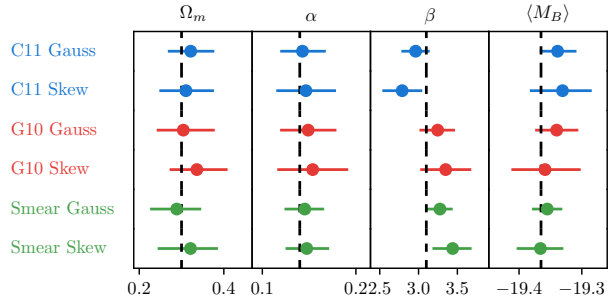

Figure 5. Parameter summaries for 20 realisations of supernova data with the Flat ΛCDM model. Discuss any biases

6 SYSTEMATICS STRENGTH TEST

systematics test

7 CONCLUSIONS

ACKNOWLEDGEMENTS

Plots of posterior surfaces and parameter summaries were created with `ChainConsumer` (Hinton 2016).

REFERENCES

Abbott T., et al., 2016, Monthly Notices of the Royal Astronomical Society, 460, 1270
Alam S., et al., 2017, Monthly Notices of the Royal Astronomical Society, 470, 2617
Amanullah R., et al., 2010, The Astrophysical Journal, 716, 712
Astier P., et al., 2006, Astronomy and Astrophysics, 447, 31
Bailey S., et al., 2008, eprint arXiv:0810.3499
Balland C., et al., 2009, Astronomy and Astrophysics, 507, 85
Barbary K., et al., 2010, The Astrophysical Journal, 745, 27
Bernstein J. P., et al., 2012, The Astrophysical Journal, 753, 152
Betoule M., et al., 2014, Astronomy & Astrophysics, 568, 32
Carpenter B., et al., 2017, Journal of Statistical Software, 76, 1
Chotard N., et al., 2011, Astronomy & Astrophysics, 529, 6
Conley A., et al., 2011, The Astrophysical Journal Supplement Series, 192, 1
Contreras C., et al., 2010, The Astronomical Journal, 139, 519
D'Andrea C. B., et al., 2011, The Astrophysical Journal, 743, 172
Dilday B., et al., 2008, The Astrophysical Journal, 682, 262
Foreman-Mackey D., Hogg D. W., Lang D., Goodman J., 2013, Publications of the Astronomical Society of Pacific, 125, 306
Freedman W. L., et al., 2009, The Astrophysical Journal, 704, 1036
Graur O., et al., 2013, The Astrophysical Journal, 783, 28
Gupta R. R., et al., 2011, ApJ, 740, 92
Guy J., et al., 2007, Astronomy and Astrophysics, 466, 11
Guy J., et al., 2010, Astronomy and Astrophysics, 523, 34
Hicken M., et al., 2009, The Astrophysical Journal, 700, 331
Hinshaw G., et al., 2013, The Astrophysical Journal Supplement Series, 208, 19
Hinton S., 2016, JOSS, 1
Hlozek R., et al., 2012, The Astrophysical Journal, 752, 79
Ivezic Z., et al., 2008, eprint arXiv:0805.2366
Jennings E., Wolf R., Sako M., 2016, eprint arXiv:1611.03087, pp 1–22
Johansson J., et al., 2013, Monthly Notices of the Royal Astronomical Society, 435, 1680
Karpenka N. V., 2015, The supernova cosmology cookbook: Bayesian numerical recipes. (`arXiv:1503.03844`), `http://arxiv.org/abs/1503.03844`
Kelly P. L., Hicken M., Burke D. L., Mandel K. S., Kirshner R. P., 2010, The Astrophysical Journal, 715, 743
Kessler R., Scolnic D., 2017, The Astrophysical Journal, 836, 56
Kessler R., et al., 2009, Publications of the Astronomical Society of the Pacific, 121, 1028
Kessler R., et al., 2015, The Astronomical Journal, 150, 172
Kowalski M., et al., 2008, The Astrophysical Journal, 686, 749
Kunz M., Bassett B., Hlozek R., 2007, Physical Review D, 75, 1
LSST Science Collaboration et al., 2009, eprint arXiv:0912.0201
Lampeitl H., et al., 2010, The Astrophysical Journal, 722, 566
Ma C., Corasaniti P.-S., Bassett B. A., 2016, Monthly Notices of the Royal Astronomical Society, 463, 1651
Malmquist K. G. 1922, Lund Medd. Ser. I, 100, 1
Mandel K. S., Wood-Vasey W. M., Friedman A. S., Kirshner R. P., 2009, The Astrophysical Journal, 704, 629
Mandel K. S., Narayan G., Kirshner R. P., 2011, The Astrophysical Journal, 731, 120
March M. C., Trotta R., Berkes P., Starkman G. D., Vaudrevange P. M., 2011, Monthly Notices of the Royal Astronomical Society, 418, 2308
March M. C., Karpenka N. V., Feroz F., Hobson M. P., 2014, Monthly Notices of the Royal Astronomical Society, 437, 3298
Mosher J., et al., 2014, The Astrophysical Journal, 793, 16
Perlmutter S., et al., 1999, The Astrophysical Journal, 517, 565
Perrett K., et al., 2012, The Astronomical Journal, 144, 59
Phillips M. M., 1993, The Astrophysical Journal, 413, L105
Planck Collaboration et al., 2013, Astronomy & Astrophysics,

571, 66
Rest A., et al., 2014, The Astrophysical Journal, 795, 44
Riess A. G., et al., 1998, The Astronomical Journal, 116, 1009
Rigault M., et al., 2013, Astronomy & Astrophysics, 560, A66
Roberts E., Lochner M., Fonseca J., Bassett B. A., Lablanche P.-Y., Agarwal S., 2017, eprint arXiv:1704.07830
Rodney S. A., et al., 2014, The Astronomical Journal, 148, 13
Rubin D., et al., 2015, The Astrophysical Journal, 813, 15
Sako M., et al., 2014, eprint arXiv:1401.3317
Scolnic D., Kessler R., 2016, The Astrophysical Journal Letters, 822
Shariff H., Jiao X., Trotta R., van Dyk D. A., 2016, The Astrophysical Journal, 827, 1
Stan Development Team 2017, PyStan: the interface to Stan, http://mc-stan.org/
Sullivan M., et al., 2010, Monthly Notices of the Royal Astronomical Society, 406, 782
Suzuki N., et al., 2012, The Astrophysical Journal, 746, 85
Tripp R., 1998, A two-parameter luminosity correction for Type IA supernovae. Vol. 331, EDP Sciences [etc.], http://adsabs.harvard.edu/abs/1998A{%}26A...331..815T
Uddin S. A., Mould J., Lidman C., Ruhlmann-Kleider V., Zhang B. R., 2017, eprint arXiv:1709.05830
Weyant A., Schafer C., Wood-Vasey W. M., 2013, The Astrophysical Journal, 764, 116
Wood-Vasey W. M., et al., 2007, The Astrophysical Journal, 666, 694

APPENDIX A: SELECTION EFFECT DERIVATION

This paper has been typeset from a TEX/LATEX file prepared by the author.